Volatile Heterometallic Precursors for the Low-Temperature Synthesis of Prospective Sodium Ion Battery Cathode Materials

Zheng Wei, Alexander S. Filatov, and Evgeny V. Dikarev*

Department of Chemistry, University at Albany, Albany, New York 12222, United States

Ⓢ Supporting Information

ABSTRACT: Heterometallic single-source precursors with a proper sodium:transition-metal ratio for nonoxide sodium ion battery cathode materials are reported. Heterometallic fluorinated β-diketonates NaM(hfac)$_3$ (M = Mn (**1**), Fe (**2**), Co (**3**), and Ni (**4**); hfac = hexafluoroacetylacetonate) have been obtained on a large scale, in high yield using a one-step reaction that employs commercially available reagents. The complexes are stable in open air and highly volatile. The mass spectrometric investigation indicates the existence of heterometallic molecules in the gas phase. The presence of heterometallic species in solutions of several solvents has been unambiguously confirmed. Heterometallic precursors were shown to exhibit clean, low-temperature decomposition in argon atmosphere that results in phase-pure perovskite fluorides NaMF$_3$, the prospective cathode materials for sodium ion batteries.

Lithium ion batteries remain the fastest growing electric power storage systems due to their high energy density and long lifespan as well as cost-effective and abuse-tolerant properties.[1,2] At the same time, dramatic developments in the next generation of electrical transportation techniques and utilization of intermittent renewable energies will require substantially greater amounts of materials to build large batteries[3] as compared to those used in small portable electronic devices. The low abundance of lithium in the earth's crust and its nonuniform geographical distribution across the world make large-scale applications of lithium ion batteries problematic.[4–6] Therefore, the development of secondary batteries based on abundant and cheap alternative elements should be considered.[7,8] Similarities between lithium and sodium electrochemistry, coupled with high abundance and low cost of the latter, are major motivations behind the research on experimental sodium ion cells.[9–12] Sodium ion intercalation and storage mechanisms are also scientifically challenging because the Na$^+$ ion is ~70% larger in radius than the Li$^+$ ion. This makes it difficult to find a suitable host material to accommodate the Na$^+$ ions and to allow their rapid and reversible insertion/extraction.

Very recently, perovskites NaMF$_3$ (M = Mn, Fe, Co, Ni) were identified as prospective oxygen-free cathode materials.[13,14] High voltage displayed by ternary fluorides can help to overcome intrinsic drawbacks of sodium ion batteries associated with a lower standard electrode potential (−2.71 V vs SHE) compared to that of lithium (−3.05 V vs SHE).[15]

Besides that, the strong M−F ionic bonds in this type of material empower its robust structure of corner-sharing [MF$_3$] matrix and ensure its stability and safety during the work cycle.[16] At the same time, the ionic character of the M−F bonds is the main reason why mixed-metal fluorides exhibit a poor electronic conductivity. Therefore, fine particles and thin films of complex fluorides that provide short conductive paths for electrons within them are required for achieving high Na$^+$ ion diffusion and improving the capacity of the cathodes. Low-temperature methods of the soft chemistry approach are ideal for obtaining particles with narrow submicrometer size distribution and compositionally homogeneous thin films. In particular, single-source precursors that offer kinetically attractive decomposition routes at moderate temperatures and permit precise control over the materials stoichiometry can be explored for the preparation of fine particles that exhibit fundamental modification in electrochemical behavior of cathode materials.

The viability of the single-source precursor approach for the low-temperature synthesis of LiMn$_2$O$_4$ spinel cathode material has recently been demonstrated.[17] We have also reported[18] that heterometallic fluorinated β-diketonates can be effectively used as single-source precursors for the synthesis of mixed-metal fluorides. Vapor-phase thermolysis of volatile fluorinated precursors PbM(hfac)$_4$ (M = Mn−Zn; hfac = hexafluoroacetylacetonate) was shown to yield nanocrystalline isomorphous phases Pb$_2$MF$_6$ that were essentially free of impurities. Herein we report isolation, characterization, and decomposition study of the volatile heterometallic single-source precursors NaM(hfac)$_3$ (M = Mn(**1**), Fe(**2**), Co(**3**), and Ni(**4**)) with a proper 1:1 metal ratio for the corresponding sodium ion battery fluoride cathode materials. For the first time, we successfully managed to assess the solid-state, solution, and gas-phase structures of heterometallic compounds. Low-temperature decomposition of the title fluorinated β-diketonates was shown to afford phase-pure NaMF$_3$ perovskites.

Heterometallic β-diketonates NaM(hfac)$_3$ (M = Mn (**1**), Fe (**2**), Co (**3**), and Ni (**4**); hfac = hexafluoroacetylacetonate) have been initially obtained in sealed evacuated ampules as sole products of the solid-state reaction between stoichiometric amounts of unsolvated homometallic sodium and divalent transition-metal diketonates:

$$Na(hfac) + M(hfac)_2 \rightarrow NaM(hfac)_3 \qquad (1)$$

Since unsolvated diketonates of divalent transition metals require special preparation and handling, another solid-state reaction was suggested that employs only commercially available starting reagents, sodium hexafluoroacetylacetonate and the corresponding anhydrous transition-metal(II) chloride:

$$3Na(hfac) + MCl_2 \rightarrow NaM(hfac)_3 + 2NaCl \qquad (2)$$
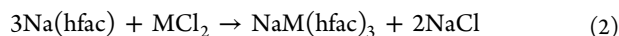
Crystals of **1–4** can be conveniently collected with ca. 88–92% yield after a few days in the cold end (5 °C temperature gradient) of the ampule, while the second product, NaCl, remains in the hot end (130–135 °C) of the container. Synthetic details for **1–4** are summarized in Tables S1–S4. Purity of the bulk diketonate products has been confirmed by X-ray powder diffraction through comparison of the experimental spectrum with the theoretical pattern calculated from the single-crystal data (Figures S1–S5).

In order to make the preparation of heterometallic precursors practical for technological applications, we suggested a solution approach for eq 2. The latter resulted in efficient preparation of **1–4** on a gram scale within few hours. The best solvent for the reaction was found to be dry, oxygen-free acetone that allows convenient separation of the diketonate products from insoluble NaCl by filtration. The solid compounds can be obtained with nearly quantitative yields by simple evaporation of the solvent under vacuum. The resulting microcrystalline products are identical to those prepared by the solid-state/gas-phase technique (Figure 1) and do not require any additional purification.
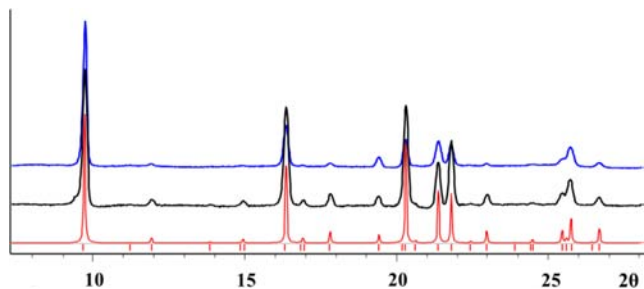

Figure 1. X-ray powder diffraction patterns of NaMn(hfac)₃ (**1**) bulk products synthesized by solution (blue) and solid-state (black) methods and their comparison with the simulated pattern (red) calculated from the single crystal data.

Heterometallic diketonates **1–4** were found to be relatively stable in moist air and can be handled outside the glovebox in a course of decomposition studies. All four compounds are highly volatile and can be purified by quantitative resublimation in a sealed ampule at 150 °C within several hours. The sublimation starts at ∼110 °C, and the compounds **1–4** do not show any traces of decomposition in evacuated ampule until 180 °C, thus displaying sufficiently large temperature window between volatility and decomposition. Heterometallic diketonates even survive in dynamic vacuum and can be efficiently purified by "cold-finger" technique at 130–140 °C for 24 h on a gram scale. Heterometallic precursors are insoluble in common noncoordinating solvents (CH_2Cl_2, $CHCl_3$, hexanes, benzene, toluene, chlorobenzene) but are readily soluble in coordinating solvents (acetone, ethanol, THF, H_2O, DMSO).

Single crystals of heterometallic diketonates suitable for X-ray structural investigation were obtained by either solvothermal method (**1** and **2**) or by slow sublimation at low temperature in

evacuated, sealed ampule placed in small temperature gradient (**3** and **4**). Single-crystal X-ray study (Table S5) revealed that heterometallic diketonates **1–4** are isomorphous, with very close parameters of a trigonal unit cell. The crystal structures contain 1D polymeric chains built on alternating Na and M(hfac)₃ units (Figures 2 and S6–S8). Transition-metal atoms
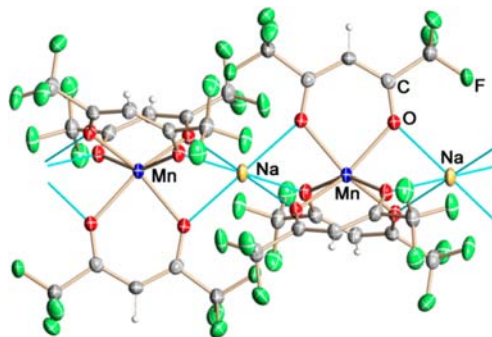

Figure 2. Fragment of the solid-state structure of NaMn(hfac)₃ (**1**) drawn with thermal ellipsoids at the 40% probability level. Na–O bonds to diketonate ligands involved in bridging interactions are shown in blue. Selected bond distances and angles for compounds **1–4** are listed in Table 1.

exhibit octahedral coordination of oxygens from three chelating diketonate ligands. Each ligand acts in a chelating-bridging mode through both oxygens thus providing distorted octahedral environment for sodium centers. The compounds can be formulated as $\{Na^+[M^{II}(hfac)_3]^-\}_\infty$ with the M–O bond lengths (Table 1) to support such an assignment. As it

**Table 1. Average Distances (Å) and Angles (°) in the Structures of Heterometallic Diketonates NaM(hfac)₃ (1–4)**

M	M–O	Na–O	M···Na	O–M–O	O–Na–O
Mn (**1**)	2.142	2.451	3.158, 3.162	84.13	71.89
Fe (**2**)	2.073	2.450	3.085, 3.086	86.51	70.97
Co (**3**)	2.066	2.446	3.133, 3.136	85.01	69.61
Ni (**4**)	2.027	2.450	3.098, 3.111	86.00	68.91

was noted before,[19] the C–H stretching frequencies of chelating-bridging diketonates in IR spectra of **1–4** (Figures S14–S17) exhibit upshift of 13–25 cm⁻¹ compared to the corresponding numbers for purely chelating ligands.

Solution structure of the title compounds was investigated in order to determine if heterometallic fragments are present in solution or the dissociation into homometallic units eventually occurs. The retention of heterometallic structure in solution is very important for evaluating the suitability of single-source precursors for the direct injection MOCVD growth of thin films. In accord with their polymeric solid-state structure, heterometallic diketonates **1–4** are insoluble in both polar and nonpolar noncoordinating solvents but readily soluble in all coordinating solvents. However, the behavior of heterometallic compounds in these solvents was found to be distinctly different. In strongly coordinating solvents like DMSO, heterometallic polymers readily dissociate into homometallic $M(hfac)_2(sol)_2$ (NMR silent) and $Na(hfac)(sol)_x$ adducts (eq 3), for which ¹H and ¹⁹F signals instantly appear in NMR spectra (Figures S18–S25).

$$[NaM(hfac)_3]_\infty + sol \rightarrow Na(hfac)(sol)_x + M(hfac)_2(sol)_2 \qquad (3)$$
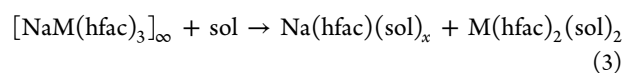
On the other hand, the solutions of **1**−**4** in less strongly coordinating, solvents, such as acetone, alcohol, and THF, are NMR (^{1}H and ^{19}F) silent. The absence of NMR signals in these solvents may indicate that the heterometallic fragments $[NaM(hfac)_3]_x$ remain intact in solution (eq 4).

$$[NaM(hfac)_3]_\infty + sol \rightarrow [NaM(hfac)_3]_x(sol)_y \qquad (4)$$
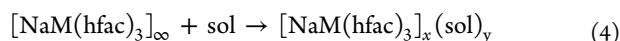
However, it can be argued that yet another dissociation pathway based on diketonate ligand redistribution may take place, also leading to NMR-silent fragments in solution:

$$[NaM(hfac)_3]_\infty + sol \rightarrow [Na(sol)_6]^+ + [M(hfac)_3]^- \qquad (5)$$
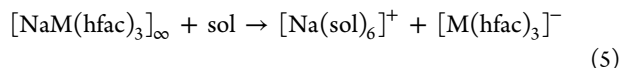
In order to account for that, we run mass spectrometric investigation of compound **1** in acetone solution. Based on our previous experience, mass spectrometric techniques were usually not informative in analysis of heterometallic diketonate species in solution due to a severe fragmentation yielding homometallic fragments. However, the use of direct analysis in real time ion source allowed us to detect the presence of complex ions in solution. Mass spectrometric investigation undoubtedly revealed the presence of heterometallic species in solution. While the positive mode is dominated by $[M + Na]^+$ species (meas/calcd 721.8858/721.8818), the negative mode features the highest peak (meas/calcd 730.8806/730.8818) corresponding to $[M + O_2]^-$ anion (M = $NaMn(hfac)_3$; O_2^- is an activator in negative mode). Several other heterometallic fragments are easily identifiable in the spectra, including those of higher nuclearity (Table S8 and Figures S10, S11).

To further test the structure of solution species, we attempted to grow the crystals from acetone mixtures. In all experiments, we managed to isolate adducts that consist of heterometallic tetramers with one or two molecules of acetone, depending on concentration of the latter (Figures 3 and S9).
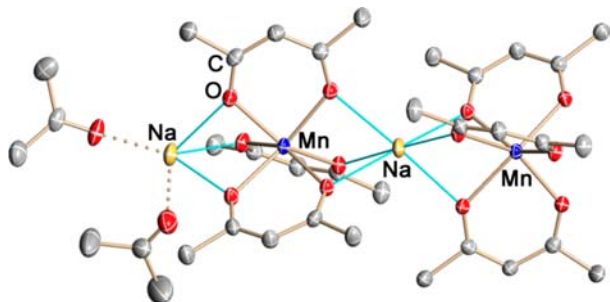

Figure 3. Crystal structure of $[NaMn(hfac)_3]_2\cdot2Me_2CO$ (**1b**) drawn with thermal ellipsoids at the 40% probability level. Bonds from sodium to oxygen atoms of acetone molecules are shown by dotted lines. All hydrogen and fluorine atoms of the CF_3 groups are omitted for clarity. Selected bond distances and angles are listed in Table S7.

The structure of solid-state species is effectively preserved in these oligomers with no diketonate ligand redistribution and acetone molecule(s) attached to the open site of coordinatively unsaturated sodium center. All the above observations unambiguously confirm the presence of heterometallic molecules in solutions of less strongly coordinating solvents.

Heterometallic diketonates **1**−**4** are highly volatile at the temperatures of ≥130 °C. Several observations indicate the presence of heterometallic species in the gas phase. First, all four precursors can be resublimed quantitatively in either static or dynamic vacuum. Second, the mass transfer of **1**−**4** in vapor

phase can be achieved at the temperatures as low as 110 °C, at which one of its possible dissociation products, Na(hfac), is not volatile. The results of mass spectrometric investigation of $NaMn(hfac)_3$ (**1**) in the gas phase strongly support the above observations. The mass spectra of heterometallic diketonate **1** were obtained at the temperatures below its decomposition point and revealed the presence of ions that are derived from heterobimetallic $NaMn(hfac)_3$ and tetrameric $Na_2Mn_2(hfac)_6$ fragments in both positive and negative modes. (Table S9 and Figures S12, S13).

According to the TGA, heterometallic diketonates **1**−**4** exhibit low-temperature decomposition that occurs in a single step ∼200 °C. TGA data (Figures S26−S29) indicate a substantial loss of mass due to volatility as a consequence of the relatively large temperature window between volatility and decomposition. Thermal decomposition of $NaM(hfac)_3$ (**1**−**4**) precursors has been carried out at different temperatures in an ambient pressure argon atmosphere oven using high alumina crucibles. The appearance of perovskite phase can be detected after just a few minutes, and $NaMF_3$ compounds can be obtained essentially free of impurities at the temperatures as low as 200 °C (Figure 4). X-ray powder diffraction analysis of
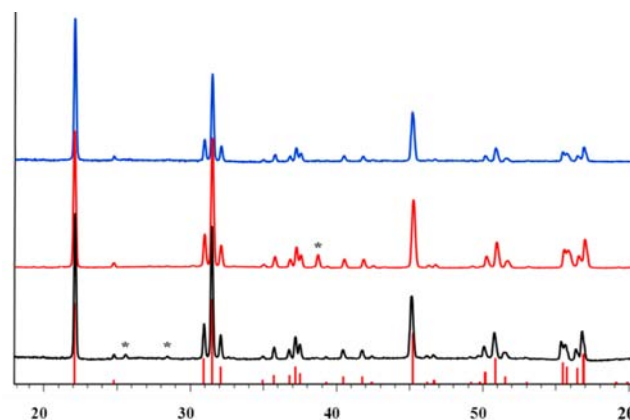

Figure 4. X-ray powder diffraction patterns of $NaMnF_3$ perovskite obtained by decomposition of $NaMn(hfac)_3$ (**1**) samples under argon at 200 °C, 2 h (black), 260 °C, 30 min (red), and 310 °C, 30 min (blue). The powder diffraction pattern corresponding to $NaMnF_3$ is shown at the bottom as a peak diagram. Impurity peaks are marked with asterisks.

decomposition traces of **1**, **3**, and **4** (Figures S30−S32) indicated that highly crystalline, phase-pure $NaMF_3$ materials were formed at 310 °C using short annealing times. Unit cell parameters for perovskite fluoride phases derived from Le Bail fit correspond well with the literature data (Table 2).

Elemental analysis revealed no appreciable carbon content in the fluoride materials. Decomposition of $NaFe(hfac)_3$ (**2**) at the above conditions resulted in oxidation of iron to Fe^{III} to yield Na_3FeF_6 fluoride. However, when thermal decomposition of heterometallic diketonate **2** has been carried out by the flash vacuum pyrolysis (FVP) method (two-zone furnace, low-pressure nitrogen flow), phase-pure $NaFeF_3$ fluoride (Figures 5 and S33) was instantly deposited. The latter experiment unambiguously confirms that $NaMF_3$ (M = Mn−Ni) perovskite materials can be obtained by vapor-phase thermolysis of the corresponding volatile heterometallic precursors.

In conclusion, heterometallic precursors **1**−**4** with a proper sodium:transition-metal ratio for prospective nonoxide sodium ion cathode materials reported in this work exhibit several

Table 2. Comparison of the Unit Cell Parameters for Tertiary Fluorides NaMF₃ Obtained by Decomposition of NaM(hfac)₃ (1−4) Precursors with the Literature Data

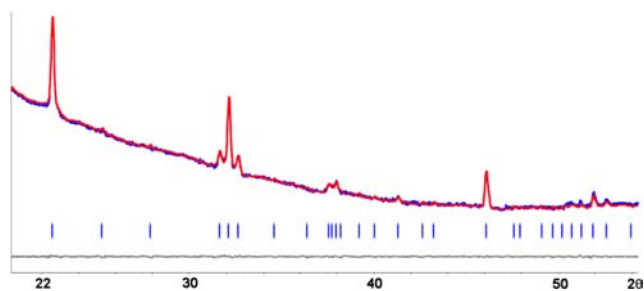| NaMF₃	literature data	Le Bail fit results
NaMnF₃[20]	*Pnma*	*Pnma*
	$a = 5.751(4)$	$a = 5.7457(2)$
	$b = 8.008(6)$	$b = 7.9990(2)$
	$c = 5.548(4)$	$c = 5.5473(2)$
	$V = 255.5(3)$	$V = 254.95(1)$
NaFeF₃[21]	*Pnma*	*Pnma*
	$a = 5.4833(11)$	$a = 5.4854(4)$
	$b = 5.6575(9)$	$b = 5.6541(5)$
	$c = 7.8754(13)$	$c = 7.8757(7)$
	$V = 244.31(7)$	$V = 244.27(4)$
NaCoF₃[22]	*Pbnm*	*Pbnm*
	$a = 5.42(3)$	$a = 5.4211(4)$
	$b = 5.60(3)$	$b = 5.6049(4)$
	$c = 7.79(3)$	$c = 7.7889(5)$
	$V = 236(2)$	$V = 236.67(3)$
NaNiF₃[23]	*Pbnm*	*Pbnm*
	$a = 5.366(1)$	$a = 5.3697(1)$
	$b = 5.530(1)$	$b = 5.5275(1)$
	$c = 7.695(1)$	$c = 7.6956(2)$
	$V = 228.34(7)$	$V = 228.41(1)$

Figure 5. X-ray powder diffraction pattern of NaFeF₃ obtained by FVP decomposition of heterometallic precursor NaFe(hfac)₃ (**2**) and the Le Bail fit for the orthorhombic unit cell (space group *Pnma*). Blue and red curves are experimental, and calculated patterns overlaid. Gray line is the difference curve. Theoretical peak positions are shown at the bottom as lines.

important characteristics of an ideal single-source precursor. Diketonate compounds are stable in moist air and can be obtained on a large scale by simple, high-yield synthetic procedure that involves only cheap, commercially available starting reagents. Volatile precursors produce heterometallic molecules in the gas phase and can be utilized in the formation of thin films of NaMF₃ cathode materials by chemical vapor deposition (CVD). The presence of heterometallic species in solution opens broad opportunities for application of the title precursors in direct liquid injection CVD techniques. Moreover, low-temperature decomposition properties of heterometallic diketonates allow preparation of the target fluoride materials in a form of nanoparticles.

■ ASSOCIATED CONTENT

Ⓢ Supporting Information

Characterization details and crystallographic file. This material is available free of charge via the Internet at http://pubs.acs.org.

■ AUTHOR INFORMATION

Corresponding Author

edikarev@albany.edu

Notes

The authors declare no competing financial interest.

■ REFERENCES

(1) Manthiram, A. *J. Phys. Chem. Lett.* **2011**, *2*, 176.
(2) Tao, H.; Feng, Z.; Liu, H.; Kan, X.; Chen, P. *Open Mater. Sci. J.* **2011**, *5*, 204.
(3) Zhang, Q.; Zhao, Y.; Su, C.; Li, M. *Recent Pat. Nanotechnol.* **2011**, *5*, 225.
(4) Jian, Z.; Zhao, L.; Pan, H.; Hu, Y.; Li, H.; Chen, W.; Chen, L. *Electrochem. Commun.* **2012**, *14*, 86.
(5) Armand, M.; Tarascon, J. M. *Nature* **2008**, *451*, 652.
(6) Zu, C.; Li, H. *Energy Environ. Sci.* **2011**, *4*, 2614.
(7) Shakoor, R. A.; Lim, S. Y.; Kim, H.; Nam, K.-W.; Kang, J. K.; Kang, K.; Choi, J. W. *Solid State Ionics* **2012**, *218*, 35.
(8) Kang, K.; Meng, Y. S.; Bréger, J.; Grey, C. P.; Ceder, G. *Science* **2006**, *311*, 977.
(9) Senguttuvan, P.; Rousse, G.; Seznec, V.; Tarascon, J. M.; Palacín, M. R. *Chem. Mater.* **2011**, *23*, 4109.
(10) Kim, D.; Kang, S.-H.; Slater, M.; Rood, S.; Vaughey, J. T.; Karan, N.; Balasubramanian, M.; Johnson, C. S. *Adv. Energy Mater.* **2011**, *1*, 333.
(11) Bhide, A.; Hariharan, K. *Solid State Ionics* **2011**, *192*, 360.
(12) (a) Whitacre, J. F.; Tevar, A.; Sharma, S. *Electrochem. Commun.* **2010**, *12*, 463. (b) Sauvage, F.; Laffont, L.; Tarascon, J. M.; Baudrin, E. *Inorg. Chem.* **2007**, *46*, 3289.
(13) Gonzalo, E.; Kuhn, A.; Garcia-Alvarado, F. *J. Electrochem. Soc.* **2010**, *157*, A1002.
(14) Gocheva, I. D.; Doi, T.; Okada, S.; Yamaki, J. *Electrochemistry* **2010**, *78*, 471.
(15) Kitajou, A.; Komatsu, H.; Chihara, K.; Gocheva, I. D.; Okada, S.; Yamaki, J. I. *J. Power Sources* **2012**, *198*, 389.
(16) Yamada, Y.; Doi, T.; Tanaka, I.; Okada, S.; Yamaki, J. I. *J. Power Sources* **2011**, *196*, 4837.
(17) Navulla, A.; Huynh, L.; Wei, Z.; Filatov, A. S.; Dikarev, E. V. *J. Am. Chem. Soc.* **2012**, *134*, 5762.
(18) Navulla, A.; Tsirlin, A. A.; Abakumov, A. M.; Shpanchenko, R. V.; Zhang, H.; Dikarev, E. V. *J. Am. Chem. Soc.* **2011**, *133*, 602.
(19) Zhang, H.; Yang, J.-H.; Shpanchenko, R. V.; Abakumov, A. M.; Hadermann, J.; Clérac, R.; Dikarev, E. V. *Inorg. Chem.* **2009**, *48*, 8480.
(20) Ratuszna, A.; Majewska, K.; Lis, T. *Acta Crystallogr.* **1989**, *C45*, 548.
(21) Benner, G.; Hoppe, R. *J. Fluorine Chem.* **1990**, *46*, 283.
(22) Rüdoff, W.; Lincke, G.; Babel, D. *Z. Anorg. Allg. Chem.* **1963**, *320*, 150.
(23) Lütgert, B.; Babel, D. *Z. Anorg. Allg. Chem.* **1992**, *616*, 133.